Solar Water Splitting

DOI: 10.1002/ange.201302680

Ordered Macroporous $BiVO_4$ Architectures with Controllable Dual Porosity for Efficient Solar Water Splitting**

Min Zhou, Hao Bin Wu, Jian Bao, Lin Liang, Xiong Wen (David) Lou, and Yi Xie**

Photoelectrochemical (PEC) water splitting based on the Fujishima–Honda effect[1] has been demonstrated as an attractive method for solar energy conversion and storage.[2] For this technology to be competitive, a crucial factor for the design of efficient photoelectrodes is to improve the utilization of charges.[3] In addition to the intrinsic nature of materials, morphology and structure also play a vital role on charge migration.[4] Hence, studies on relationships between geometrical characteristics and charge migration are very important for solar water splitting.

Among many architectures for photoelectrodes, periodically ordered macroporous structures (POMS) have attracted increasing attention for many interesting properties derived from their special structural features.[5] As shown in Scheme 1 a, the geometrical characteristics of periodically ordered macroporous structures are mainly determined by two parameters. One is the diameter of macropores surrounded by the final skeletal walls (denoted as D1). The other is the diameter of pores between neighboring macropores (denoted as D2). Both D1 and D2 will exert their influence on various processes in PEC water splitting.[6] Many reports have confirmed that the relative sizes of D1 and D2 have full influence on light absorption, deriving from the shift of the photonic stop band.[6a,7a] Lee et al. also mentioned that the proper D1 size would lead to efficient electron drift mobility.[7b] However, the influence of dual porosity on charge migration, which originates from, for example, different charge transport channels, grain size, surface states, has long been neglected. A possible reason for this deficiency is the lack of synthetic control over dual pore sizes. The difficulties mainly stem from the requirements of meeting the following three factors simultaneously. First, controllable templates with plasticity of the diameter and the interconnected area between neighboring spheres are required to adjust D1 and D2. Second, a proper infiltration method with higher infiltration fraction of precursors is needed to maintain topological transformation from the template. Lastly, the method should be versatile for various attractive materials.

Inspired by above considerations, we highlight herein a general solution approach to tackle the challenge via a modified colloidal crystal templating method. Different from previous strategies, the combination of a sandwich solution infiltration strategy and a post-heating treatment of template greatly benefits both the structural and compositional controllability, and therefore, provides a platform for understanding correlations between geometrical characteristics and PEC properties. As a proof of concept, we choose $BiVO_4$ as a model material to study the relationship between dual pore sizes in periodically ordered macroporous structures and charge migration process during PEC water splitting. $BiVO_4$ has been shown to be highly efficient for PEC water splitting, but still suffers primarily from some problems of inefficient charge migration according to theoretical and experimental studies.[8]

Fabrication of such architectures with designed features is achievable as outlined in Scheme 1 a. Owing to the high degree of periodicity in three dimensions, the template can be translated into the replica periodically ordered macroporous structure topologically. During this transformation, if the diameter of the spheres can be controlled and the contact area between neighboring spheres, it is in principle feasible to control the sizes of D1 and D2 in the final structure. We choose monodispersed polystyrene (PS) spheres as the unit in view of their easily adjustable diameter and more importantly plasticity resulting from the low glass transition temperature.[9] With the increased post- heating time, PS spheres will deform continuously so that the contact between neighboring PS spheres can evolve from no contact to point contact, and finally to quasi-face contact (Scheme 1 b). This will give rise to tunable geometrical features of the final architectures with the help of high filling fraction to efficiently realize topological transformation. However, a high filling fraction of precursor is difficult to achieve through common solution infiltration methods.[6a] In view of the above, we propose a novel sandwich-like configuration for infiltration as illustrated in Scheme 1 b to realize higher filling fraction of precursor solution. Specifically, the template is confined between two substrates, one of which is hydrophilic and the other is hydrophobic. A support (spacer) layer with a thickness slightly larger than that of the template is inserted between the two substrates. During the infiltration process, the lower edge of the whole sandwich-like structure is

[*] Dr. M. Zhou, J. Bao, L. Liang, Prof. Y. Xie
Hefei National Laboratory for Physical Sciences at the Microscale
Department of Chemistry
University of Science & Technology of China
Hefei, Anhui 230026 (P.R. China)
E-mail: yxie@ustc.edu.cn
H. B. Wu, Prof. X. W. Lou
School of Chemical and Biomedical Engineering
Nanyang Technological University
62 Nanyang Drive, 637459 (Singapore)
E-mail: xwlou@ntu.edu.sg
Homepage: http://www.ntu.edu.sg/home/xwlou/

[**] This work was financially supported by National Basic Research Program of China (2009CB939901), the Chinese Academy of Sciences (XDB01020300), and National Nature Science Foundation (11079004, 90922016).

Supporting information for this article is available on the WWW under http://dx.doi.org/10.1002/anie.201302680.

© 2013 Wiley-VCH Verlag GmbH & Co. KGaA, Weinheim

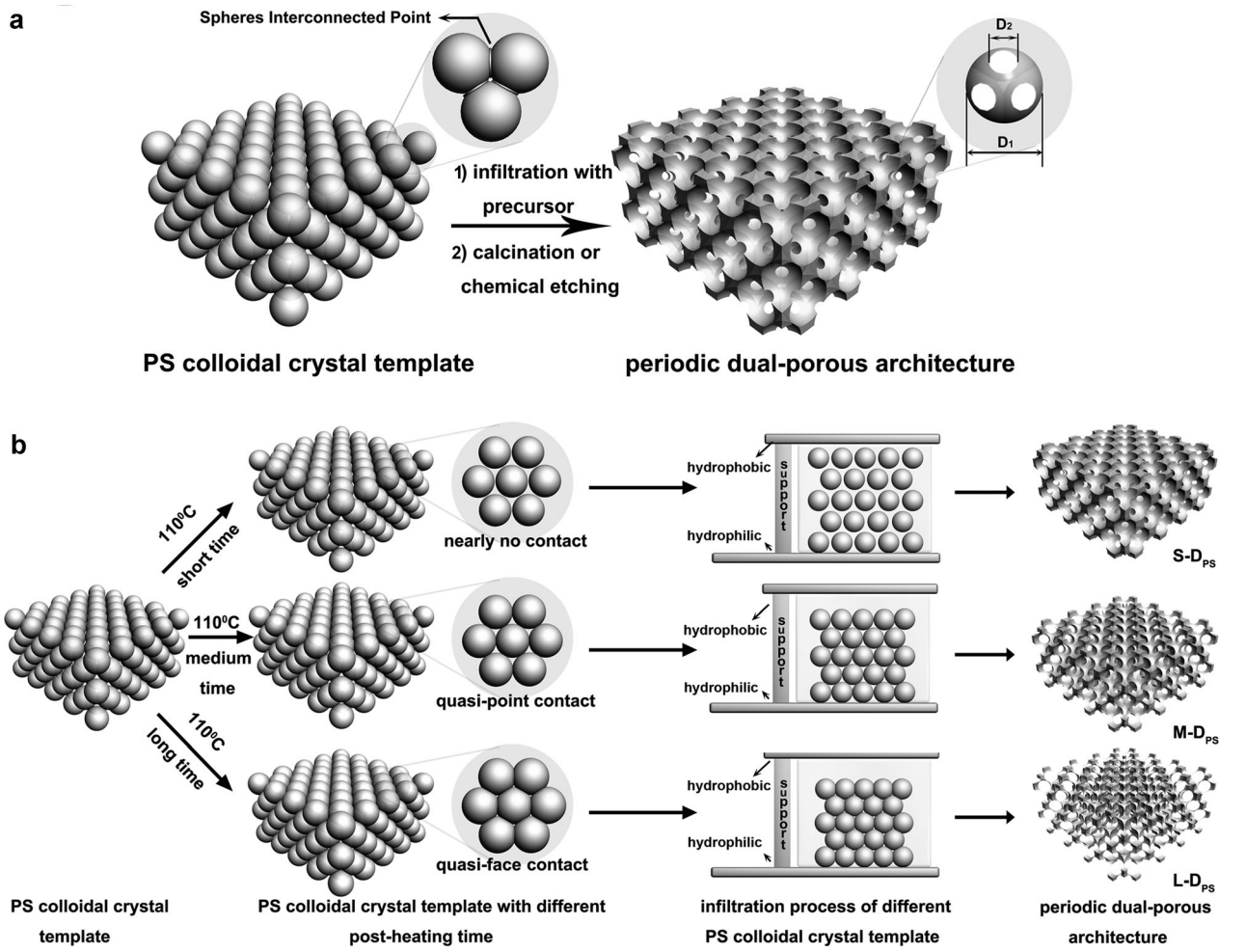

Scheme 1. a) A schematic representation of the dual porosity in periodic ordered porous architectures. D1: diameter related to that of sphere. D2: diameter related to interconnected point between spheres. b) Schematic illustration of the approach for controlling D2 in periodic ordered porous architectures.

immersed into the precursor solution vertically, so that solution can penetrate into the interstices of the template.[10] The bottom substrate is hydrophilic so that the precursor solution can infiltrate easily, especially around the interface between the template and substrate; while the top substrate is hydrophobic, therefore the intermediate composite can be prevented from adhering to this substrate and the integrity of the as-obtained architecture is maintained. Furthermore, the support between two different substrates allows a local space for the template spheres to suspend and disperse as much as possible without structural collapse. With a short post-heating time and hence less deformation of the PS spheres, the extended distance between adjacent spheres enables more solution to enter the interstitial space, and thus the filling fraction of precursor solution is increased while maintaining the structural integrity. Therefore, the two major parameters of geometrical characteristics within the as-obtained architectures can be adjusted. D1 is mainly determined by the diameter of PS spheres, and D2 is controlled by the contact surface-to-volume ratio which is changed by the post-heating time. Our goal of controllable dual porosity can be achieved through the combination of the post-heating treatment and the sandwich solution infiltration method.

To implement aforementioned concepts, we performed the post-heating treatment on the colloidal crystal template assembled from 200 nm PS spheres at 110 °C for different durations from S (short, 0 min) to M (medium, ca. 3–5 min) and L (long, ca. 10–12 min). Clearly shown in Figure 1 a–c and Figure S1a in the Supporting Information, with continuous deformation caused by heating, the contact between neighboring PS spheres gradually changes from nearly no contact to point contact to quasi-face contact, and finally to face contact. This induced deformation by heating is general for PS spheres with different diameters, such as 420 nm in Figure 1 d–f and Figure S1b, 1000 nm in Figure 1 g–i and Figure S1c. Then all the templates are infiltrated with proper precursor solution of $BiVO_4$ by the sandwich solution infiltration method.

As expected, periodically ordered macroporous structures of phase-pure $BiVO_4$ (Figure S2, see Supporting Information) with controllable dual pore sizes are prepared as shown in Figure 2. A careful observation reveals that D1 is mainly

© 2013 Wiley-VCH Verlag GmbH & Co. KGaA, Weinheim

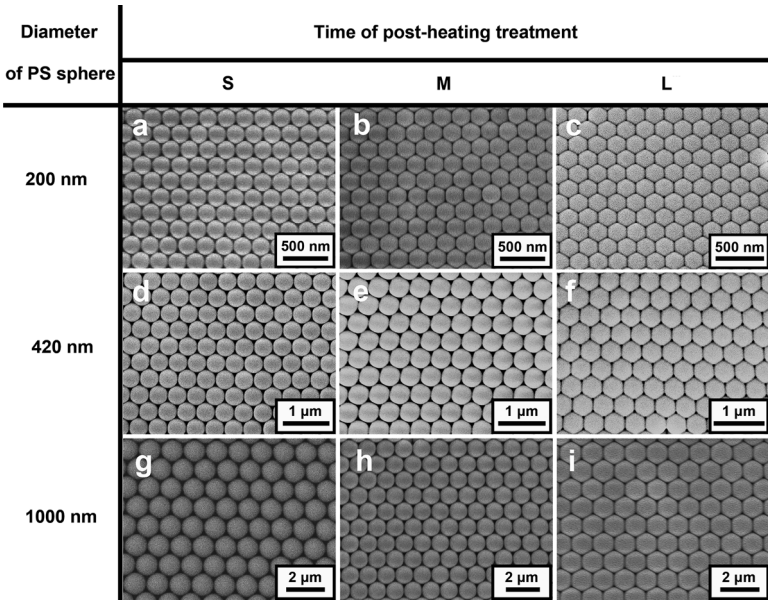

Figure 1. The deformation of the PS spheres template after post-heating treatment for different durations. The diameter of the PS spheres is a)–c) 200 nm. d)–f) 420 nm. g)–i) 1000 nm. Note: for S the post-heating time of the template is 0 min for samples shown in (a), (d), and (g). For M the post-heating time of template is 3 min for the sample shown in (b) and 5 min for samples shown in (e) and (h). For L the post-heating time of template is 10 min for samples shown in (c) and (f), and 12 min for the sample shown in (i).

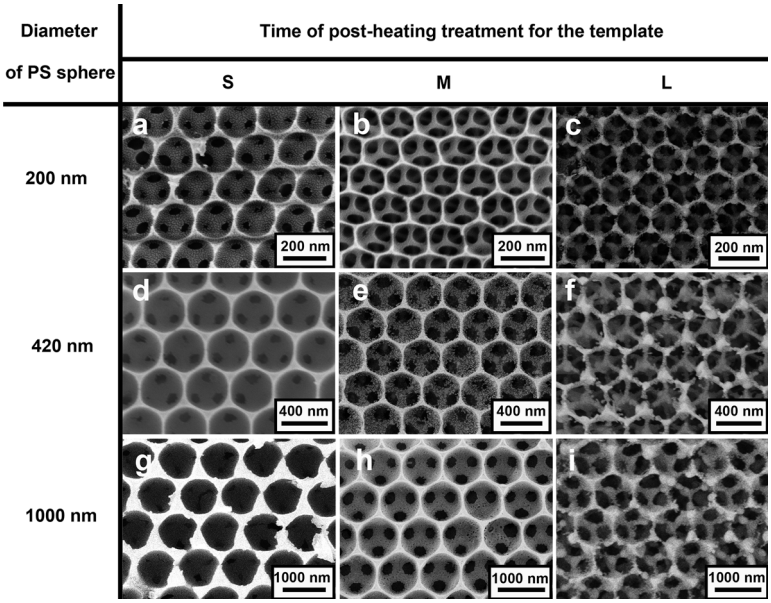

Figure 2. Typical SEM images of corresponding $BiVO_4$ periodically ordered porous architectures with controllable dual porosity. a) S-200, b) M-200, c) L-200, d) S-420, e) M-420, f) L-420, g) S-1000, h) M-1000, i) L-1000. The diameter of original PS spheres is a)–c) 200 nm. d)–f) 420 nm. g)–i) 1000 nm. For S the post-heating time of the template is 0 min for samples shown in (a), (d), and (g). For M, the post-heating time of the template is 3 min for the sample shown in (b) and 5 min for samples shown in (e) and (h). For L, the post-heating time of the template is 10 min for samples shown in (c) and (f), and 12 min for the sample shown in (i).

related to the diameter of original PS spheres, which is still valid when using templates with different post-heating times. Note that the well-defined macropores in the top layer connect to the corresponding macropores in the sub-layer through the necks. The diameter of interconnected area (D2) is directly associated with the post-heating time of templates. For convenience, hereafter, we designate various periodically ordered macroporous structures as "X-D_{PS}", where X refers to the post heating duration (S, M, or L) and D_{PS} is the diameter of PS spheres in nanometer. The positive effects of the sandwich infiltration strategy are: If the top surface is not hydrophobic, the surface of as-obtained samples would be rugged (Figure S3) because some PS spheres would adhere to the substrate and then be separated from the template when removing the top substrate. Moreover, if the hydrophobic substrate and the support are not used to make a local space, the template would straggle easily during the infiltration of precursor solution. As a result, the final structures obtained will not be so periodically ordered (Figure S4). Besides, the wall of the periodically ordered macroporous structure becomes thinner with increased post-heating time, showing another direct consequence of various D2 derived from the increased deformation of PS spheres and higher filling fraction. All the above evidence verifies the structural designs illustrated in Scheme 1. The morphology and structure are dependent more on the template rather than the type of precursor solution. The premise of the present approach lies in the fact that the wettability is guaranteed, hence the precursor solution could be arbitrarily chosen. Similar periodically ordered macroporous structures with controllable dual pore sizes can be easily fabricated for many other materials, including binary materials, such as Bi_2O_3 (Figure S5), ternary materials such as LiV_3O_8 (Figure S6), Bi_2WO_6 (Figure S7). In addition, controllable doping for different composition and concentration can also be easily realized, such as Mo-doped $BiVO_4$ (Figure S8). From this perspective, such a solution approach is of great importance in providing structural and compositional controllability and a better understanding of the correlations between structure and performance.

To probe the resulting effects on charge migration for water splitting, PEC cells were fabricated using various samples from templates of 200 nm and 1000 nm PS spheres with different post-heating times. Because all the samples have been optimized to share similar calculated maximum photocurrent densities ($J_{abs} \approx 5.0\ mA\,cm^{-2}$ under 1 sun AM 1.5 sunlight, details are provided in Section S2), it could be asserted that the difference in the photocurrent densities (J) can be fully ascribed to the difference in photon utilization, which directly depends on charge migration in bulk and on surface. As summarized in Table 1 (also in Figure S9a, S10a), analysis

 © 2013 Wiley-VCH Verlag GmbH & Co. KGaA, Weinheim

Table 1: Relationship between PEC performance and dual porosity.

Sample	D1 [nm]	D2 [nm]	J @ 0.4 V/ mA cm^{-2} [a]	J @ 1.2 V/ mA cm^{-2} [a]	R_{ct} [Ω]	Photoelectron lifetime @ 0.6 V/s [b]
S-200	180	35 ± 5	0.38	1.35	268.7	2.01
M-200	170	85 ± 5	0.30	0.84	350.0	1.82
L-200	155	105 ± 5	0.29	0.64	762.3	1.62
S-1000	850	105 ± 5	0.25	0.80	1187	1.70
M-1000	780	150 ± 5	0.22	0.65	1621	1.54
L-1000	710	560 ± 5	0.13	0.55	2815	1.31

[a] The voltage is referenced to Ag/AgCl. [b] The voltage is referenced to RHE.

of the photocurrent densities on various samples allows us to make the following two observations. 1) All the photoelectrodes achieve much higher photocurrent density over unordered porous film (only 0.3 mA cm^{-2} at 1.2 V vs. Ag/AgCl; Figure S11). This result implies that periodically ordered macroporous skeleton is indeed advantageous as a photoelectrode. 2) Carefully analyzing the curves of samples from templates with PS spheres of the same diameter, we find that the enhancement under a higher voltage bias is more pronounced with shorter post-heating times. It is established that bulk charge recombination is the main limiting factor with the increased bias.[8a,11] Therefore, this apparent enhancement suggests that a smaller D2 is beneficial for suppressing charge recombination, and hence easier charge migration.

In essence, the hypothesis we want to verify is that the existence of smaller D2 within the $BiVO_4$ periodically ordered porous architectures can facilitate charge migration. At least two types of measurements can be conducted to study the effects of D2. The first one is based on the assumption that the interface charge transfer kinetics can be measured by electrochemical impedance spectroscopy (EIS). As presented in Figure S9b and S10b, the Nyquist plots consist of one dominant semicircle, whose diameter is related to charge transfer resistance at $BiVO_4$/electrolyte interface.[12] Comparing samples with identical D1 but different D2, samples with smaller D2 lead to a smaller diameter of the semicircle. To further understand the details, we interpret the plots in terms of the equivalent circuit using the Randles–Ershler model displayed in the inset of Figure S9b and S10b, where R_{ct} represents the charge transfer resistance across the interface. As listed in Table 1, the fitted values of R_{ct} clearly show that the interface charge transfer in samples of smaller D2 is much easier.

The second technique to appreciate the advantages of smaller D2 relies on how it affects bulk charge migration behavior. Shown in Figure S9c and S10c is the open circuit voltage decay among the samples with different D2 values. On one hand, the observation of the slightly negative shift of the open circuit voltage (V_{oc}) with less post-heating time indicates that the D2 size has an important impact on the process occurring at the interface, that is, a smaller D2 means larger junction area.[13] If the flux of photo-generated charges is instead distributed uniformly over a much larger junction area, the bulk recombination limit would be reduced, associated with improved surface reactions and hole interface transfer. Although increased junction area would also result in an increased rate of surface recombination, effective suppression on bulk recombination contributes more to the enhanced charge migration and hence PEC performance.[14] On the other hand, under illumination, the steady-state charge-carrier concentrations at the junction set the position of the quasi-Fermi levels, which in turn determines V_{oc}. Conversely, under transient conditions when the illumination is stopped, more inner defects and boundaries become preferable sites where electrons and holes are easy to recombine.[15] As such, a faster V_{oc} decay would be observed immediately after the removal of illumination. With the help of the methodology by Bisquert et al.,[16] we find that the V_{oc} decay in L-D_{PS} is faster than in S-D_{PS} (insets of Figure S9c, S10c). Furthermore, the V_{oc} decay rate is related to the photoelectron lifetime.[16b] With shortened post-heating time (Table 1), the photoelectron lifetime is correspondingly prolonged (Section S3, see Supporting Information). Slower decay kinetics and longer photoelectron lifetime are indicative of less charge trapping when illuminated, hence, more effective charge separation for water splitting.[15]

Meanwhile, when comparing the PEC performance of L-200 and S-1000 which have similar D2 values, the tendency of enhanced photocurrent density with increased D1 is very different under low and high bias voltages. As for L-200, a slightly higher photocurrent at the lower bias indicates that smaller D1 enables suppression of surface recombination and easy interface charge transfer, which is evidenced by smaller R_{ct}. The S-1000 sample exhibits a higher photocurrent density at the higher bias. This observation together with higher photoelectron lifetime verifies that increased D1 benefits the elimination of bulk charge recombination.

As seen from above characterizations, the $BiVO_4$ periodically ordered macroporous structures with different dual porosity offer multiple effects. Specifically, smaller D2 is helpful for charge migration both in bulk and on surface, while smaller D1 facilitates surface charge migration, but impedes bulk charge migration. They can be further rationalized: 1) A more compact space occupation of samples with smaller D1 and D2 results in larger electrode/electrolyte junction area, which ensures higher electrode/electrolyte area and more active sites to reduce resistance at interface/charge transfer resistance and open circuit voltage. It can be expected that there are more holes capable of surviving the recombination and then reaching the electrode/electrolyte interface for further utilization. Accordingly, more electrons can be collected by the current collector. 2) With respect to samples with smaller D2 and larger D1, the thickness of the wall increases, leading to more interfacial contact between electrode materials and the current collector. So the contact resistance can be minimized and charge transfer at the electrode/current collector interface is facilitated.[4a] 3) It can be imagined that the thin wall formed within the interstitial spaces generated by smaller PS spheres is much more fragile during the calcination process. With D1 being constant, a more compact packing or smaller grain size of $BiVO_4$ grains in the interstitial space can be achieved by introducing a smaller D2. The opposite situation occurs while keeping D2

© 2013 Wiley-VCH Verlag GmbH & Co. KGaA, Weinheim

constant and introducing smaller D1. Therefore, there will be less inner defects and grain boundaries, which usually serve as charge recombination centers, by having small D1 and large D2 in the periodically ordered macroporous structures. This situation will benefit charge transfer in the bulk of the photoelectrode.[7b] Overall, the above evidence and analysis support the hypothesis that the periodically ordered macroporous structures with different dual porosity play a vital role in charge migration. Being able to apply a similar level of synthetic control over dual porosity to various materials offers the potential to ease charge migration problems in PEC water splitting. Although only one J_{abs} is considered, the observed effects of dual pore size should be general. Hence, it is believed that our findings will shed some light for further development of efficient photoelectrodes for PEC cells.

In summary, we have demonstrated a general solution approach to fabricate periodically ordered porous architectures with control over dual porosity based on a modified colloidal crystal templating method. As a proof of concept, $BiVO_4$ was used as a model material to investigate the influences of geometrical features on charge migration for PEC water splitting. A series of measurements, including PEC characterizations, electrochemical impedance measurements, and open-circuit voltage decay, have verified that charge migration in the $BiVO_4$ periodically ordered macroporous architectures shows strong dependence on the relative size of dual porosity. Under the conditions of approximately 5.0 mA cm^{-2} (J_{abs}) under 1 sun AM 1.5 sunlight, a smaller D2 value is beneficial for charge migration both in the bulk and on the surface, while a smaller D1 value facilitates surface charge migration but impedes the bulk charge migration. This finding can serve as a guideline for further design of photoelectrodes with high efficiency.

Received: April 1, 2013
Published online: June 14, 2013

Keywords: charge migration · colloidal crystal templates · dual periodic porosity · photoelectrochemistry

[1] A. Fujishima, K. Honda, *Nature* **1972**, *238*, 37.
[2] a) M. Grätzel, *Nature* **2001**, *414*, 338; b) M. G. Walter, E. L. Warren, J. R. McKone, E. A. Santori, N. S. Lewis, *Chem. Rev.* **2010**, *110*, 6446.
[3] C. Liu, Y. J. Hwang, H. E. Jeong, P. Yang, *Nano Lett.* **2011**, *11*, 3755.
[4] a) M. Zhou, J. Bao, Y. Xie, *Chem. Commun.* **2012**, *48*, 3362; b) K. Sivula, F. Le Formal, M. Grätzel, *ChemSusChem* **2011**, *4*, 432.
[5] a) G. von Freymann, V. Kitaev, B. V. Lotsch, G. A. Ozin, *Chem. Soc. Rev.* **2013**, *42*, 2528; b) K. A. Arpin, A. Mihi, H. T. Johnson, A. J. Baca, J. A. Rogers, J. A. Lewis, P. V. Braun, *Adv. Mater.* **2010**, *22*, 1084.
[6] a) L. Liu, S. K. Karuturi, A. I. Y. Tok, *Energy Environ. Sci.* **2011**, *4*, 209; b) J. Du, X. Lai, N. Yang, J. Zhai, D. Kisailus, F. Su, D. Wang, L. Jiang, *ACS Nano* **2011**, *5*, 590; c) J. Du, X. Lai, J. E. Halpert, Y. Yang, D. Wang, *Sci. China Chem.* **2011**, *54*, 930.
[7] a) C. Cheng, S. K. Karuturi, L. Liu, J. Liu, H. Li, L. T. Su, A. I. Y. Tok, H. J. Fan, *Small* **2012**, *8*, 37; b) E. S. Kwak, W. Lee, N. G. Park, J. Kim, H. Lee, *Adv. Funct. Mater.* **2009**, *19*, 1093.
[8] a) M. Zhou, J. Bao, W. Bi, Y. Zeng, R. Zhu, M. Tao, Y. Xie, *ChemSusChem* **2012**, *5*, 1420; b) W. Luo, Z. Yang, Z. Li, J. Zhang, J. Liu, S. Yan, T. Yu, Z. Zou, *Energy Environ. Sci.* **2011**, *4*, 4046.
[9] Y. Li, W. Cai, B. Cao, G. Duan, C. Li, F. Sun, H. Zeng, *J. Mater. Chem.* **2006**, *16*, 609.
[10] J. H. Moon, S. Yang, *Chem. Rev.* **2010**, *110*, 547.
[11] H. Gao, C. Liu, H. E. Jeong, P. Yang, *ACS Nano* **2012**, *6*, 234.
[12] B. Klahr, S. Gimenez, F. Fabregat-Santiago, T. Hamann, J. Bisquert, *J. Am. Chem. Soc.* **2012**, *134*, 4294.
[13] J. R. Maiolo, H. A. Atwater, N. S. Lewis, *J. Phys. Chem. C* **2008**, *112*, 6194.
[14] B. M. Kayes, H. A. Atwater, N. S. Lewis, *J. Appl. Phys.* **2005**, *97*, 114302.
[15] Y. Lin, Y. Xu, M. T. Mayer, Z. I. Simpson, G. McMahon, S. Zhou, D. Wang, *J. Am. Chem. Soc.* **2012**, *134*, 5508.
[16] a) A. Zaban, M. Greenshtein, J. Bisquert, *ChemPhysChem* **2003**, *4*, 859; b) Z. Zhang, P. Wang, *Energy Environ. Sci.* **2012**, *5*, 6506.

© 2013 Wiley-VCH Verlag GmbH & Co. KGaA, Weinheim